Thymosin β10 mediates the effects of microRNA-184 in the proliferation and epithelial-mesenchymal transition of BCPAP cells

CHENG YANG[1*], YUNNI LIU[1*] and KUN FANG[2]

[1]Department of Thyroid and Breast Surgery, The Central Hospital of Wuhan, Wuhan, Hubei 430014; [2]Department of Surgery, Yinchuan Women and Children's Hospital, Yinchuan, Ningxia Hui Autonomous Region 750004, P.R. China

Received September 30, 2020; Accepted March 15, 2021

DOI: 10.3892/etm.2021.10174

Abstract. Thyroid cancer is the most common malignant tumor of the endocrine system. It has been reported that thymosin β10 (TMSB10) serves a vital role in tumor invasion and metastasis, and further understanding the role of TMSB10 in thyroid cancer may provide new insights into the development of novel targeted drugs. Bioinformatics analysis suggested that there might exist a regulatory relationship between miR-184 and TMSB10. Therefore, the expression of microRNA (miR)-184 was investigated in the TPC-1 and BCPAP thyroid cancer cell lines and the Nthy-ori 3-1 thyroid epithelial cell line via reverse transcription-quantitative PCR. The effect of miR-184 on BCPAP cell proliferation was evaluated using MTT and colony formation assays. In addition, the expression levels of epithelial-mesenchymal transition (EMT)-associated proteins were examined via western blot analysis and immunofluorescence staining. Furthermore, the targeting association between miR-184 and TMSB10 was verified using a dual-luciferase reporter assay. Notably, miR-184 overexpression attenuated BCPAP cell proliferation, increased the expression level of the epithelial marker E-cadherin, and decreased that of the mesenchymal marker vimentin. These effects were reversed in BCPAP cells following TMSB10 overexpression. The present study revealed that TMSB10 may be considered as a key mediator in promoting papillary thyroid carcinoma (PTC) cell proliferation and EMT, which were negatively regulated by miR-184. Therefore, the findings of the present study may provide a novel potential therapeutic target for attenuating PTC cell proliferation.

Correspondence to: Dr Kun Fang, Department of Surgery, Yinchuan Women and Children's Hospital, 56 Wenhua West Street, Yinchuan, Ningxia Hui Autonomous Region 750004, P.R. China
E: mail: fangkunf@126.com

*Contributed equally

Key words: thyroid tumor, thymosin β10, microRNA-184, epithelial-mesenchymal transition

Introduction

Thyroid cancer is the most prevalent malignant tumor of the endocrine system (1). Globally, there has been an increase by 20% in the age-standardized incidence rate of thyroid cancer, with a minimal alteration in the mortality rates (2,3). Understanding the pathogenesis of thyroid cancer is crucial for improving and appropriately tailoring diagnostic and therapeutic strategies. MicroRNAs (miRNAs/miRs) act by blocking mRNA translation or inducing mRNA degradation through interactions with complementary sequences in the 3'-untranslated regions (3'-UTRs) of their target mRNA transcripts (4,5). It has been reported that several miRNAs, such as, miR-214 and miR-451a, can act upstream of different proteins in papillary thyroid carcinoma (PTC), thereby regulating PTC cell growth (6-8). A recent study has demonstrated that the differential expression of mRNAs and miRNAs was closely associated with metastasis in PTC (9). Additionally, another study has revealed that miR-184 could regulate nasopharyngeal cancer cell invasion and epithelial-mesenchymal transition (EMT) (10). In addition, a previous study has suggested that oxidized miR-184 was involved in facilitating cell apoptosis (11). EMT serves a key role in the metastasis and invasion of malignant tumors, whereby epithelial cells lose their adhesive ability and acquire the migratory ability of mesenchymal cells (12-14).

The results of the UALCAN database (http://ualcan.path.uab.edu/index.html) (15) revealed that the expression level of thymosin β10 (TMSB10) was upregulated in thyroid cancer tissues compared with that in normal tissues (data not shown). It has been previously demonstrated that the mRNA expression level of TMSB10 differed significantly between normal thyroid tissues and PTC, with or without lymph node metastasis (LNM), and the increased expression level of TMSB10 was associated with LNM in PTC (16), suggesting that TMSB10 may serve a key role in PTC. Furthermore, TMSB10 knockout has been indicated to inhibit the migratory and invasive ability of renal carcinoma cells *in vitro* (17). TMSB10 has also been revealed to be upregulated in breast cancer cells and tissues, while TMSB10 silencing attenuates the proliferation, invasion and migration of breast cancer cells *in vitro* and *in vivo* (18). However, the upstream targets and

the mechanism underlying the role of TMSB10 in PTC remain largely unknown. Therefore, further elucidation of the effects of TMSB10 in thyroid cancer may enable the development of novel targeted drugs for this type of cancer.

Materials and methods

Cells. The human PTC cell line TPC-1, the poorly differentiated thyroid gland carcinoma cell line BCPAP, which has been verified by short tandem repeat profiling, and the normal thyroid epithelial cell line Nthy-ori 3-1 were all purchased from American Type Culture Collection. Cells were cultured in RPMI-1640 medium containing penicillin (100 U/ml), streptomycin (0.1 mg/ml) and supplemented with 10% FBS (both from Gibco; Thermo Fisher Scientific, Inc.) at 37˚C in a 5% CO_2 incubator.

Cell transfection. BCPAP cells were harvested using trypsin and then seeded into 12-well plates at a density of $1x10^6$ cells/well. Cells were transfected with 50 nM miR-184 mimics (5'-UGGACGGAGAACUGAUAAGGGU-3') or negative control (NC) mimics (mimic-NC; 5'-UGACGGCAU GUGAUAGAGAAGG-3'), (Guangzhou RiboBio Co., Ltd.) TMSB10 overexpression plasmid (pcDNA-TMSB10; 0.2 μg; Miaoling Biological Technology Co., Ltd.) or pcDNA (empty vector, 0.2 μg) using Lipofectamine® 2000 (Invitrogen; Thermo Fisher Scientific, Inc.) for 24 h at 37˚C, according to the manufacturer's instructions. The cells were then used for further experiments.

Reverse transcription-quantitative (RT-q)PCR analysis. Total RNA was extracted from cells with TRIzol® reagent (Thermo Fisher Scientific, Inc.) and cDNA was synthesized using a Transcriptor Hi-Fi cDNA Synthesis kit (Sigma-Aldrich; Merck KGaA). The temperature protocol was 25˚C for 5 min, 42˚C for 30 min and 85˚C for 5 min. Following PCR amplification, RNA was quantitatively analyzed according to the instructions of the TaqMan One Step PCR kit (Beijing Solarbio Science & Technology Co., Ltd.). The cycling conditions of PCR were pre-denaturation at 95˚C for 2 min, followed by a total of 40 cycles of 95˚C for 30 sec, 60˚C for 35 sec, 72˚C for 1 min. The relative levels of miR-184 or TMSB10 mRNA were calculated using $2^{-\Delta\Delta Cq}$ method (19). β-actin and U6 served as the internal references for mRNA and miRNA, respectively. The primers used for PCR were designed using Primer3 Input software (version 0.4.0; https://primer3.ut.ee) and synthesized by Sangon Biotech Co., Ltd. The primers used were: miR-184 forward: 5'-TACGACTATGTGACCTGCCTG-3', reverse 5'-TGGTTCAACTCTCCTTTCCA-3'. TMSB10 forward: 5'-GAAATCGCCAGCTTCGATAAGG-3', reverse 5'-TCA ATGGTCTCTTTGGTCGGC-3' U6 forward, 5'-TGCTGG GGCTTTCCGGCAGCGC-3' and reverse, 5'-CCCAGTGAG GTCCGGAGGT-3'. β-actin: Forward: 5'-CTCGCCTTTGCC GATCC-3', 5'-GGGGTACTTCAGGGTGAGGA-3'.

MTT assay. BCPAP cells were cultured into a 96-well plate at a cell density of $2x10^4$ cells/well. Following transfection, 10 μl MTT reagent was added into each well and the cells were incubated for an additional 4 h at 37˚C. Subsequently, 150 μl DMSO was added to each well and mixed at a low speed on a shaking bed to dissolve formazan crystals. The absorbance at 570 nm was measured using a microplate reader.

Colony formation assay. BCPAP cells in the logarithmic growth phase were cultured in 6-cm culture dishes at a density of $1x10^3$ cells/dish. The culture medium was replaced every 2 days. Following culture for 2 weeks, the formed colonies (>50 cells) visible to the naked eye were observed under a microscope and the culture was then terminated. Cells were rinsed thrice in D-Hank's Balanced Salt Solution (D-HBSS; Thermo Scientific, Inc.), fixed in 4% paraformaldehyde for 20 min at room temperature and stained with 0.1% crystal violet solution at room temperature for 20 min. Subsequently, the cells were washed again three times with D-HBSS, and then observed in five random fields under a light microscope.

Immunofluorescence (IF) staining. Briefly, BCPAP cells in the logarithmic growth phase were seeded into 24-well plates ($5x10^5$ cells), fixed in 4% paraformaldehyde at room temperature for 10 min, and were subsequently incubated with 1% Triton X-100 for 10 min at room temperature. Following blocking with 2% BSA (Beijing Solarbio Science & Technology Co., Ltd.) for 30 min at room temperature, the cells were incubated with primary antibodies (anti-E-cadherin; cat. no. ab231303; 1:500 and anti-vimentin; cat. no. ab8978; 1:100; Abcam) at 4˚C overnight. The primary antibodies were then discarded, and cells were incubated with corresponding secondary antibodies (goat polyclonal secondary antibody to rabbit IgG, cat. no. ab150084; goat secondary antibody to Mouse IgG; cat. no. ab150117; 1:1,000; Abcam) at 37˚C for 1 h. Subsequently, the cells were treated with a DAPI staining solution at room temperature in the dark for 10 min, followed by washing three times with PBS. Finally, the cells were observed, and images were captured under an inverted fluorescence microscope (Olympus Corporation, magnification, x200).

Western blot analysis. Total proteins in each group were extracted with a RIPA buffer (Beyotime Institute of Biotechnology) and the protein concentration was measured using a BCA kit (Beyotime Institute of Biotechnology). The protein concentration in each group was adjusted, and protein samples (50 μg) were separated via 10% SDS-PAGE and then transferred onto PVDF membranes. Following blocking with 5% skimmed milk for 2 h at room temperature, the membranes were incubated with the appropriate concentration of the primary antibody (anti-E-cadherin; cat. no. ab231303; 1:500; anti-vimentin, cat. no. ab8978; 1:500; ZEB1; cat. no. ab203829; 1:500; GAPDH; cat. no. ab8245; 1:1,000; all from Abcam) at 4˚C overnight. On the following day, the membranes were washed with PBS for 5 min and then incubated with the corresponding secondary antibody (goat anti-mouse IgG; cat. no. ab97040; goat anti-rabbit IgG; cat. no. ab7090; 1:10,000; Abcam) for 1 h at room temperature. A color-developing solution (Super ECL Detection Reagent kit; Shanghai Yeasen Biotechnology Co., Ltd.) was then added, followed by exposure in a dark room. Images of protein strips were captured using a gel imaging system (Bio-Rad Laboratories, Inc.). The grey value of the protein bands was evaluated with ImageJ 1.46r software (National Institutes of Health). GAPDH was used as an internal reference.

Bioinformatics analysis. StarBase database (http://starbase.sysu.edu.cn/) was searched for the prediction of relationship between miR-184 and TMSB10. The database revealed potential binding sites of miR-184 in the 3'-UTR of TMSB10.

Dual-luciferase reporter assay. Transfection experiments were carried out using Lipofectamine 2000 according to the manufacturer's protocol. Luciferase plasmids (pGL3-basic; Promega Corporation) encompassing wild-type or mutant TMSB10 3'-UTR were co-transfected into BCPAP cells with miR-184 mimic or mimic-NC. At 6 h following transfection, the transfection medium was replaced with complete RPMI culture medium. Following incubation for 48 h, the luciferase activity was determined using Dual-Glo® Luciferase Assay System (Promega Corporation). Finally, the luminescence intensity was measured using a microplate reader [Tecan (Shanghai) Trading Co., Ltd.]. *Renilla* luciferase was used to be as internal reference.

Statistical analysis. One-way ANOVA was utilized to determine the significance among multiple groups using GraphPad Prism software (version 7.0; GraphPad Software, Inc.), followed by Tukey's post hoc test. The experimental data are presented as the mean ± SD. Each experiment was repeated at least three times. $P<0.05$ was considered to indicate a statistically significant difference.

Results

miR-184 overexpression attenuates BCPAP cell proliferation. The expression level of miR-184 in the thyroid cancer cell lines BCPAP and TPC-1 and in the normal thyroid epithelial cell line Nthy-ori 3-1 was determined via RT-qPCR, and the results demonstrated that miR-184 expression was most significantly decreased in BCPAP cells (Fig. 1). It has been reported that the expression level of miR-184 was markedly downregulated in patients with thyroid cancer compared with healthy controls and was positively associated with overall survival (20,21). Therefore, the BCPAP cell line was selected for the subsequent mechanistic experiments. BCPAP cells were transfected with miR-184 mimics or mimic-NC. At 48 h following transfection, miR-184 expression was increased in cells treated with miR-184 mimics (Fig. 2A). To evaluate cell proliferation, MTT assays were carried out at 24, 48 and 72 h after transfection of BCPAP cells with miR-184 mimics. As presented in Fig. 2B, BCPAP cells overexpressing miR-184 exhibited reduced proliferative ability compared with cells in the mimic-NC or control groups (cells receiving no treatment. (Fig. 2B). Additionally, miR-184 overexpression reduced the colony formation ability of BCPAP cells compared with the mimic-NC and control groups (Fig. 2C).

miR-184 overexpression suppresses EMT. To further characterize the effects of miR-184 at the molecular level, BCPAP cells were transfected with miR-184 mimics, and the expression of the EMT markers E-cadherin and vimentin was detected via IF analysis. The results demonstrated that miR-184 overexpression notably increased the expression levels of E-cadherin and decreased those of vimentin compared with the mimic-NC and control groups (Fig. 3A and B). In addition,

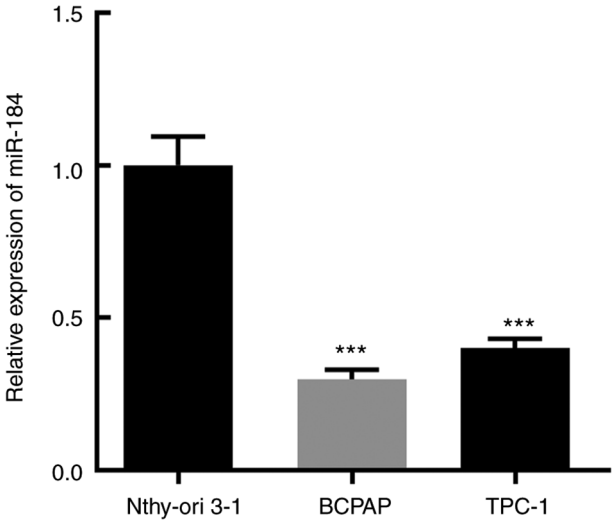

Figure 1. Detection of miR-184 expression levels in normal and cancer thyroid cell lines via reverse transcription-quantitative PCR. The experimental data are presented as the mean ± SD. ***$P<0.001$ vs. Nthy-ori 3-1. miR, microRNA.

western blot analysis revealed that miR-184-overexpressing cells displayed significantly increased E-cadherin and decreased vimentin and zinc finger E-box-binding homeobox 1 (ZEB1) expression levels compared with those in the control and mimic-NC groups (Fig. 3C).

miR-184 directly targets TMSB10 3'-UTR. The aforementioned findings suggested that miR-184 was downregulated in BCPAP cells. Subsequently, the mRNA and protein levels of TMSB10 were detected in different thyroid cancer cell lines. The results demonstrated that the expression level of TMSB10 was increased in BCPAP cells compared with Nthy-ori 3-1 normal thyroid epithelial cell line, suggesting a possible association between miR-184 and TMSB10 (Fig. 4A and B). Subsequently, it was examined whether the expression of TMSB10 could be regulated by miR-184. Mutations of five bases were generated in the potential binding site of miR-184 in the TMSB10 3'-UTR. Co-transfection of BCPAP cells with the wild-type TMSB10 3'-UTR luciferase plasmids and miR-184 mimics resulted in decreased luciferase activity compared with the mimic-NC group (Fig. 4C). No significant difference was observed in luciferase activity between the cotransfection group of mutant-type TMSB10 3'-UTR luciferase plasmids and miR-184 mimics and the mimic-NC group. In addition, miR-184 mimics notably decreased the mRNA and protein expression levels of TMSB10 compared with the mimic-NC or control groups (Fig. 4D and E). Taken together, the aforementioned findings suggested that the regulation of TMSB10 expression could be partially mediated by miR-184.

miR-184 regulates the effects of TMSB10. RT-qPCR results demonstrated that transfection of BCPAP cells with pcDNA-TMSB10 markedly increased the TMSB10 mRNA expression level compared with empty vector or control cells (Fig. 5A). To further evaluate the effects of TMSB10 and the regulatory mechanism of miR-184, the cell proliferation rate and the expression of EMT-associated markers was

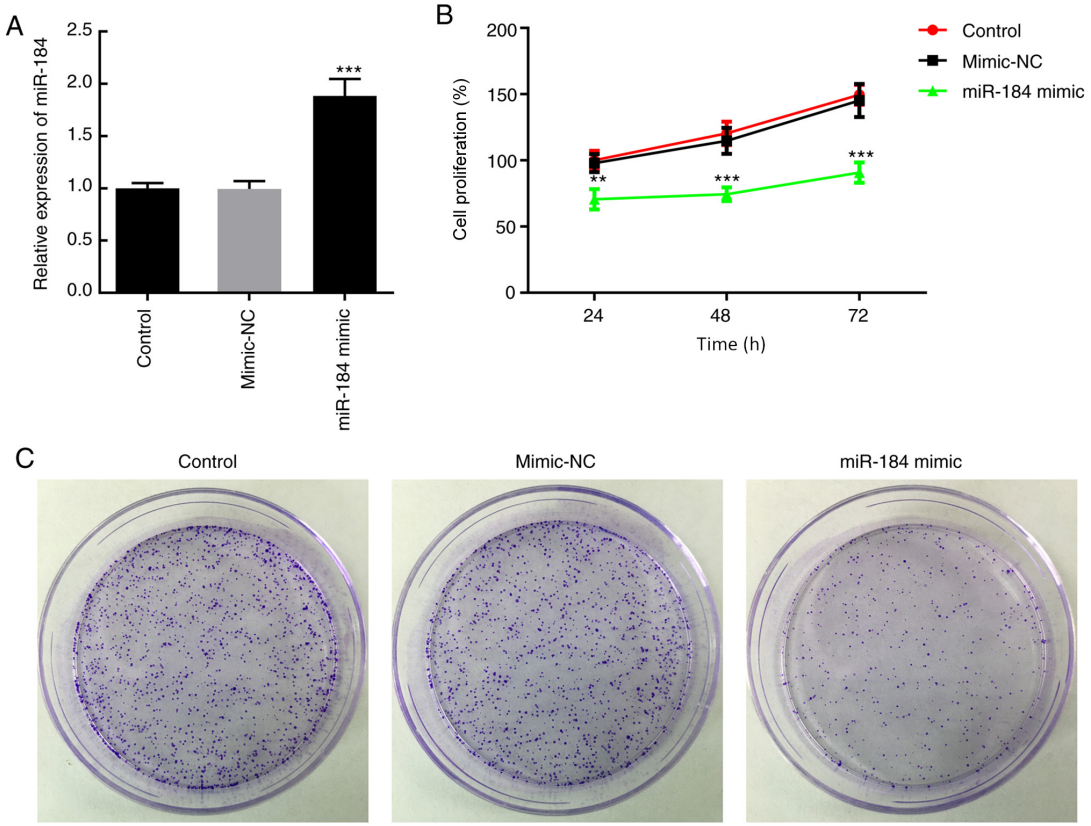

Figure 2. miR-184 overexpression suppresses the proliferation of BCPAP cells. (A) Expression of miR-184 was upregulated following transfection with miR-184 mimics for 48 h. (B) MTT assay demonstrating BCPAP cell proliferation following transfection of BCPAP cells with miR-184 mimic or mimic-NC for 24, 48 or 72 h. (C) Colony formation ability was determined using a colony formation assay. The experimental data are presented as the mean ± SD. **P<0.01, ***P<0.001. miR, microRNA; NC, negative control.

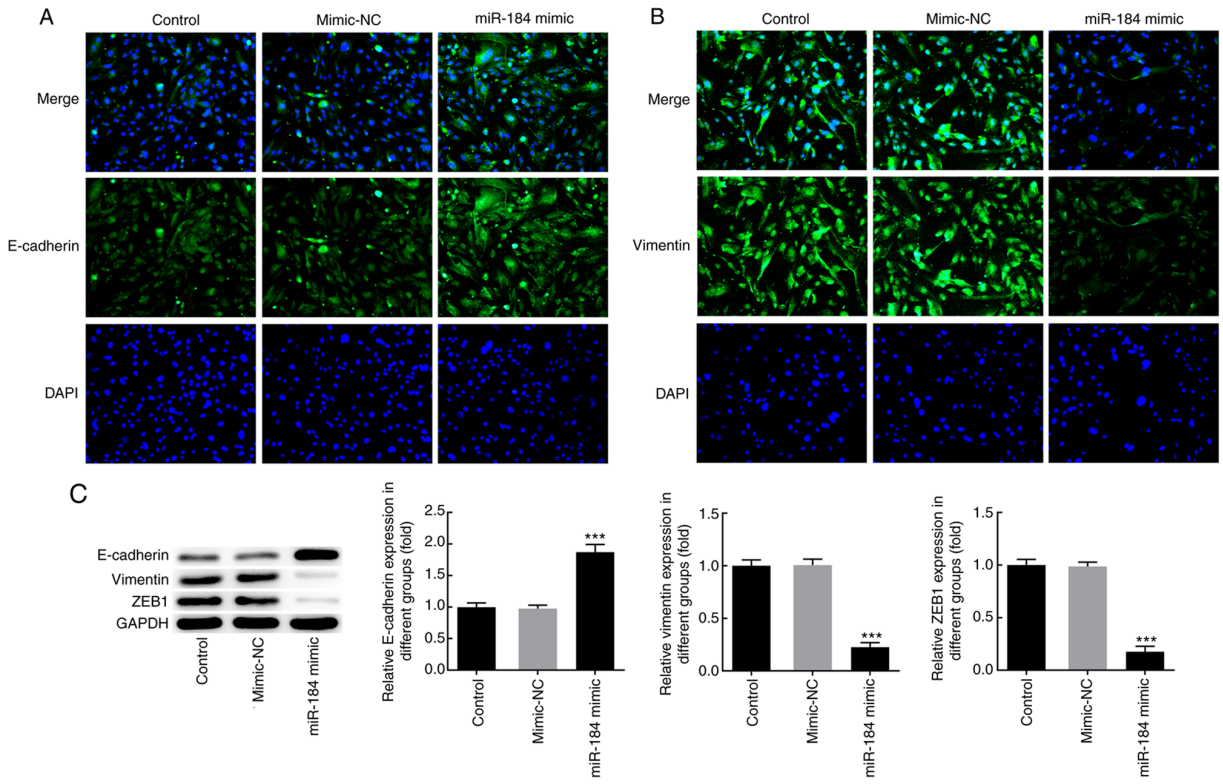

Figure 3. miR-184 overexpression alters the expression of E-cadherin, vimentin and ZEB1. Immunofluorescence staining of (A) E-cadherin and (B) vimentin after transfection of miR-184 mimics for 48 h. (C) Expression levels of E-cadherin, vimentin and ZEB1 were detected by western blot analysis. The experimental data are presented as the mean ± SD. Magnification, x200. ***P<0.001. ZEB1, zinc finger E-box-binding homeobox 1; miR, microRNA; NC, negative control.

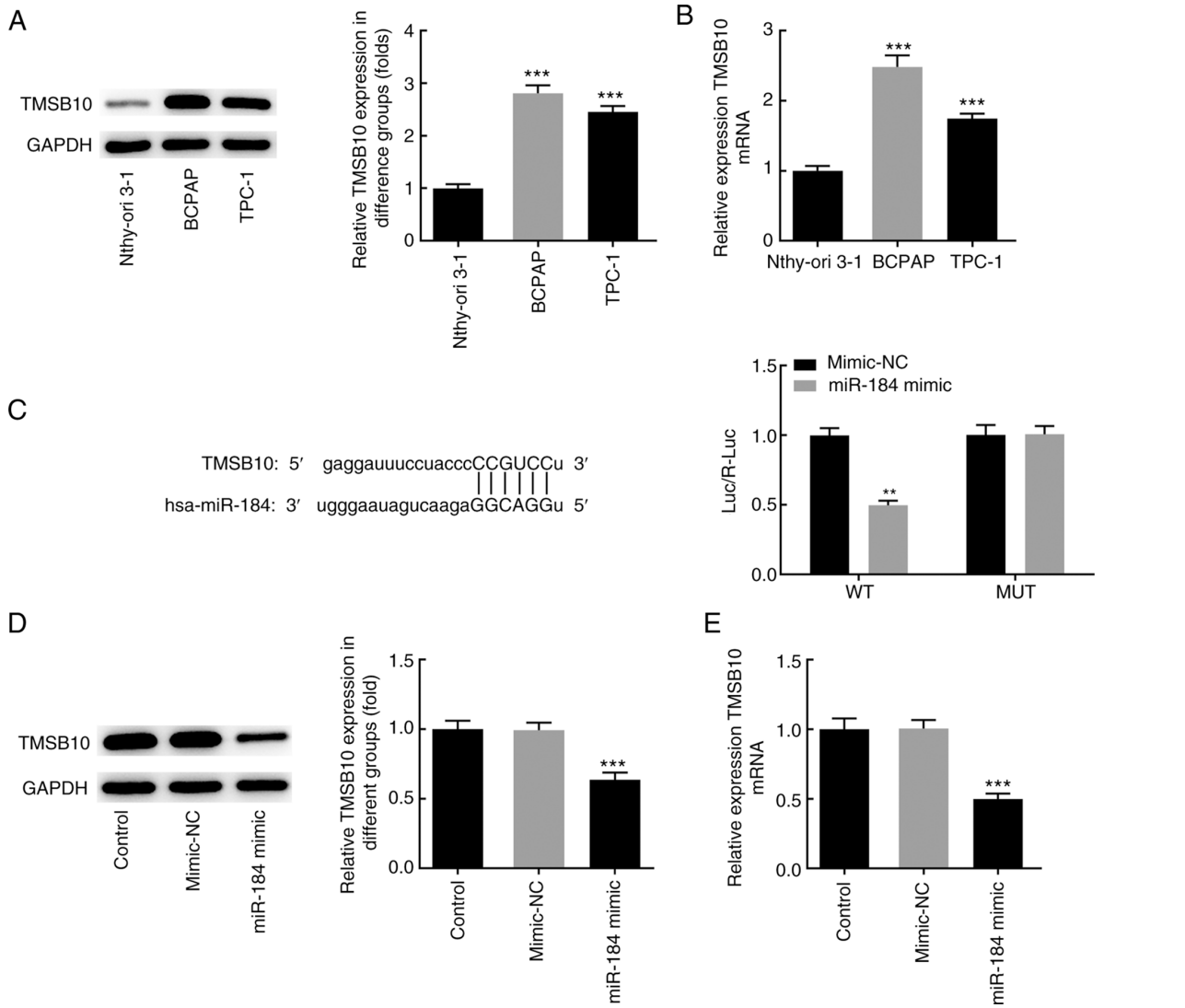

Figure 4. TMSB10 expression was detected via (A) western blot and (B) reverse transcription-quantitative PCR analyses in Nthy-ori 3-1, BCPAP and TPC-1 cells. (C) Luciferase reporter assay was conducted to verify the direct targeting of TMSB10 by miR-184; the bases in uppercase letters indicate the complementary region between TMSB10 and miR-184. Cell transfection with miR-184 mimics for 48 h markedly reduced the (D) protein and (E) mRNA expression level of TMSB10. The experimental data are presented as the mean ± SD. **P<0.01, ***P<0.001. TMSB10, thymosin β10; miR, microRNA; NC, negative control; WT, wild-type; MUT, mutant.

determined in BCPAP cells overexpressing miR-184 and TMSB10. Of note, TMSB10 overexpression reversed the effects of miR-184 overexpression on cell proliferation, colony formation and expression of EMT markers (Fig. 5B-F). These findings collectively indicated that alterations in the expression of miR-184 may result in increased TMSB10 levels in thyroid cancer, thereby promoting thyroid cancer cell proliferation and EMT.

Discussion

The present study demonstrated that miR-184 overexpression could markedly reduce TMSB10 expression in BCPAP cells, indicating that decreased miR-184 expression levels may contribute to upregulated TMSB10 expression in BCPAP cells. It has been previously demonstrated that TMSB10 was upregulated in squamous cell carcinoma and its upregulated levels were not considered to be due to its hypomethylation status; however, this mechanism was not considered as the main mechanism underlying TMSB10 upregulation (22). In the present study, TMSB10 mediated the effects of miR-184 on thyroid cancer cell proliferation and EMT. TMSB10, which is an actin-sequestering protein belonging to the β-thymosin family, has been associated with LNM in PTC (15). Additionally, it has been reported that TMSB10 promotes the malignant behavior of breast cancer cells, and is therefore considered to be a potential therapeutic target in breast cancer (18).

In breast cancer cells, TMSB10 has been observed to promote cell proliferation and invasion via the AKT/FOXO signaling pathway (22). In addition, several studies have reported that TMSB10 expression is closely associated with disease progression and unfavorable prognosis in different types of cancer, such as hepatocellular carcinoma and bladder cancer (23,24). EMT is an important process involved in normal embryonic development, and is a key factor in tumor invasion and metastasis (25), which is characterized by loss of cell adhesion, downregulation of E-cadherin expression and enhanced cell mobility (26). Immunostaining results on the expression of vimentin and

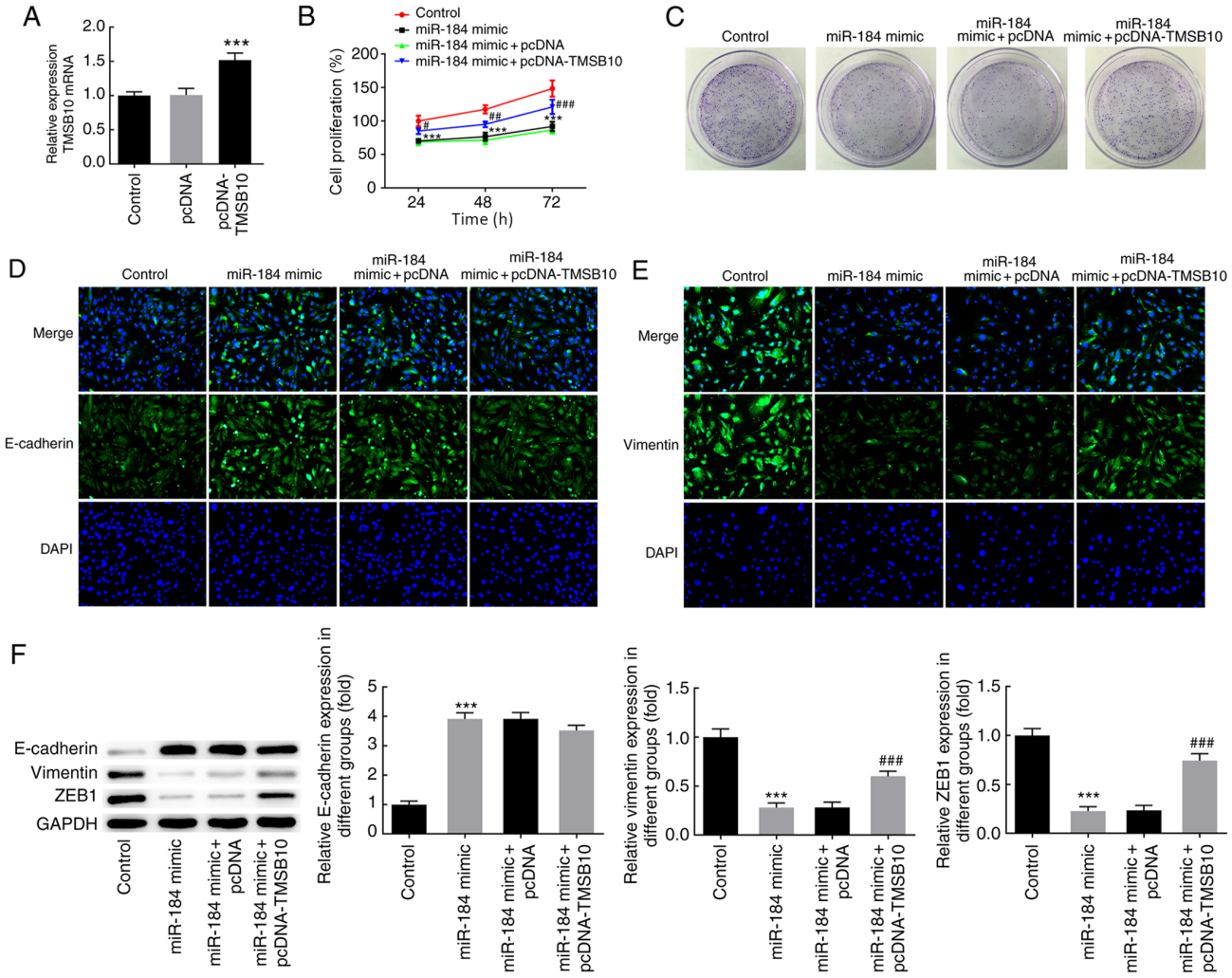

Figure 5. miR-184 regulated the expression of TMSB10. (A) TMSB10 mRNA expression following cell transfection with pcDNA-TMSB10. ***P<0.001 vs. pcDNA. (B) Cell proliferation was evaluated using an MTT assay. #P<0.05, ##P<0.01, ###P<0.001 vs. miR-184 mimic + pcDNA at 24, 48 and 72 h, respectively. ***P<0.001 vs. control at 24, 48 and 72 h, respectively. (C) Colony formation assay following cell transfection with miR-184 mimics and pcDNA-TMSB10. Immunofluorescence staining demonstrating the protein expression of (D) E-cadherin and (E) vimentin. (F) Protein expression of E-cadherin, vimentin and ZEB1 as determined by western blot analysis, ***P<0.001 vs. control; ###P<0.001 vs. miR-184 mimic + pcDNA. The experimental data are presented as the mean ± SD. Magnification, x200. TMSB10, thymosin β10; ZEB1, zinc finger E-box-binding homeobox 1; miR, microRNA; NC, negative control.

E-cadherin indicated that the expression levels of both proteins were closely associated with the size and progression of thyroid tumors (27). ZEB1 is a key molecule in EMT, directly binding to the E-box element via its zinc finger domain and suppressing the transcription of the CDH1 gene, which encodes E-cadherin protein; ZEB1 has been indicated to promote EMT, invasion and metastasis of thyroid cancer cells (28,29).

In the present study, miR-184 overexpression in BCPAP cells upregulated E-cadherin expression levels, and downregulated vimentin and ZEB1 expression levels, suggesting that miR-184 may suppress EMT. Notably, TMSB10 overexpression partly restored the effects of miR-184 overexpression on BCPAP cells. An increasing number of studies have focused on the regulation of EMT in thyroid cancer, shedding light on its pathogenesis, and various signaling pathways have been associated with the regulation of EMT (30-32). The present study highlighted the potential regulatory effect of the miR-184/TMSB10 axis on EMT in thyroid cancer. The regulatory role of the miR-184/TMSB10 axis in cell proliferation and EMT requires further validation *in vivo*, which is a limitation of the present study and a further research direction. To the best of our knowledge, the present study is the first to report the regulatory role of TMSB10 in human thyroid cancer and provide preliminary findings on its underlying mechanism of action, thereby indicating a potential novel target for inhibiting the proliferation of thyroid cancer cells.

Acknowledgements

Not applicable.

Funding

No funding was received.

Availability of data and materials

The datasets used and/or analyzed during the current study are available from the corresponding author on reasonable request.

Authors' contributions

CY, YL and KF made substantial contributions to the conception and design of the study, performed the experiments, interpreted the data and drafted and revised the manuscript for important intellectual content. CY and KF confirm the authenticity of the raw data. All authors read and approved the final manuscript.

Ethics approval and consent to participate

Not applicable.

Patient consent for publication

Not applicable.

Competing interests

The authors declare that they have no competing interests.

References

1. Davies L and Welch HG: Current thyroid cancer trends in the United States. JAMA Otolaryngol Head Neck Surg 140: 317-322, 2014.
2. Roman BR, Morris LG and Davies L: The thyroid cancer epidemic, 2017 perspective. Curr Opin Endocrinol Diabetes Obes 24: 332-336, 2017.
3. Cabanillas ME, McFadden DG and Durante C: Thyroid cancer. Lancet 388: 2783-2795, 2016.
4. Luo L, Xia L, Zha B, Zuo C, Deng D, Chen M, Hu L, He Y, Dai F, Wu J, *et al*: miR-335-5p targeting ICAM-1 inhibits invasion and metastasis of thyroid cancer cells. Biomed Pharmacother 106: 983-990, 2018.
5. Li R, Teng X, Zhu H, Han T and Liu Q: MiR-4500 regulates PLXNC1 and inhibits papillary thyroid cancer progression. Horm Cancer 10: 150-160, 2019.
6. Liu F, Lou K, Zhao X, Zhang J, Chen W, Qian Y, Zhao Y, Zhu Y and Zhang Y: miR-214 regulates papillary thyroid carcinoma cell proliferation and metastasis by targeting PSMD10. Int J Mol Med 42: 3027-3036, 2018.
7. Minna E, Romeo P, Dugo M, De Cecco L, Todoerti K, Pilotti S, Perrone F, Seregni E, Agnelli L, Neri A, *et al*: miR-451a is underexpressed and targets AKT/mTOR pathway in papillary thyroid carcinoma. Oncotarget 7: 12731-12747, 2016.
8. Qiu Z, Li H, Wang J and Sun C: miR-146a and miR-146b in the diagnosis and prognosis of papillary thyroid carcinoma. Oncol Rep 38: 2735-2740, 2017.
9. Condello V, Torregrossa L, Sartori C, Denaro M, Poma AM, Piaggi P, Valerio L, Materazzi G, Elisei R, Vitti P and Basolo F: mRNA and miRNA expression profiling of follicular variant of papillary thyroid carcinoma with and without distant metastases. Mol Cell Endocrinol 479: 93-102, 2019.
10. Zhu HM, Jiang XS, Li HZ, Qian LX, Du MY, Lu ZW, Wu J, Tian XK, Fei Q, He X and Yin L: miR-184 inhibits tumor invasion, migration and metastasis in nasopharyngeal carcinoma by targeting Notch2. Cell Physiol Biochem 49: 1564-1576, 2018.
11. Wang JX, Gao J, Ding SL, Wang K, Jiao JQ, Wang Y, Sun T, Zhou LY, Long B, Zhang XJ, *et al*: Oxidative modification of miR-184 enables it to target Bcl-xL and Bcl-w. Mol Cell 59: 50-61, 2015.
12. Zheng X, Carstens JL, Kim J, Scheible M, Kaye J, Sugimoto H, Wu CC, LeBleu VS and Kalluri R: Epithelial-to-mesenchymal transition is dispensable for metastasis but induces chemoresistance in pancreatic cancer. Nature 527: 525-530, 2015.
13. Da C, Wu K, Yue C, Bai P, Wang R, Wang G, Zhao M, Lv Y and Hou P: N-cadherin promotes thyroid tumorigenesis through modulating major signaling pathways. Oncotarget 8: 8131-8142, 2017.
14. Lv N, Shan Z, Gao Y, Guan H, Fan C, Wang H and Teng W: Twist1 regulates the epithelial-mesenchymal transition via the NF-κB pathway in papillary thyroid carcinoma. Endocrine 51: 469-477, 2016.
15. Chandrashekar DS, Bashel B, Balasubramanya SAH, Creighton CJ, Rodriguez IP, Chakravarthi BVSK and Varambally S: UALCAN: A portal for facilitating tumor subgroup gene expression and survival analyses. Neoplasia 19: 649-658, 2017.
16. Zhang XJ, Su YR, Liu D, Xu DB, Zeng MS and Chen WK: Thymosin beta 10 correlates with lymph node metastases of papillary thyroid carcinoma. J Surg Res 192: 487-493, 2014.
17. Xiao R, Shen S, Yu Y, Pan Q, Kuang R and Huang H: TMSB10 promotes migration and invasion of cancer cells and is a novel prognostic marker for renal cell carcinoma. Int J Clin Exp Pathol 12: 305-312, 2019.
18. Zhang X, Ren D, Guo L, Wang L, Wu S, Lin C, Ye L, Zhu J, Li J, Song L, *et al*: Thymosin beta 10 is a key regulator of tumorigenesis and metastasis and a novel serum marker in breast cancer. Breast Cancer Res 19: 15, 2017.
19. Livak KJ and Schmittgen TD: Analysis of relative gene expression data using real-time quantitative PCR and the 2(-Delta Delta C(T)) method. Methods 25: 402-408, 2001.
20. Tang J, Kong D, Cui Q, Wang K, Zhang D, Yuan Q, Liao X, Gong Y and Wu G: Bioinformatic analysis and identification of potential prognostic microRNAs and mRNAs in thyroid cancer. PeerJ 6: e4674, 2018.
21. Xu Y, Chen J, Yang Z and Xu L: Identification of RNA expression profiles in thyroid cancer to construct a competing endogenous RNA (ceRNA) Network of mRNAs, Long noncoding RNAs (lncRNAs), and microRNAs (miRNAs). Med Sci Monit 25: 1140-1154, 2019.
22. Lee SM, Na YK, Hong HS, Jang EJ, Yoon GS, Park JY and Kim DS: Hypomethylation of the thymosin β(10) gene is not associated with its overexpression in non-small cell lung cancer. Mol Cells 32: 343-348, 2011.
23. Song C, Su Z and Guo J: Thymosin β10 is overexpressed and associated with unfavorable prognosis in hepatocellular carcinoma. Biosci Rep 39: BSR20182355, 2019.
24. Wang B, Wang Z, Zhang T and Yang G: Overexpression of thymosin β10 correlates with disease progression and poor prognosis in bladder cancer. Exp Ther Med 18: 3759-3766, 2019.
25. Paolillo M and Schinelli S: Extracellular matrix alterations in metastatic processes. Int J Mol Sci 20: 4947, 2019.
26. Pradella D, Naro C, Sette C and Ghigna C: EMT and stemness: Flexible processes tuned by alternative splicing in development and cancer progression. Mol Cancer 16: 8, 2017.
27. Calangiu CM, Simionescu CE, Stepan AE, Cernea D, Zăvoi RE and Mărgăritescu C: The expression of CK19, vimentin and E-cadherin in differentiated thyroid carcinomas. Rom J Morphol Embryol 55: 919-925, 2014.
28. Morillo-Bernal J, Fernandez LP and Santisteban P: FOXE1 regulates migration and invasion in thyroid cancer cells and targets ZEB1. Endocr Relat Cancer 27: 137-151, 2020.
29. Xia W and Jie W: ZEB1-AS1/miR-133a-3p/LPAR3/EGFR axis promotes the progression of thyroid cancer by regulating PI3K/AKT/mTOR pathway. Cancer Cell Int 20: 94, 2020.
30. Li T, Zhao N, Lu J, Zhu Q, Liu X, Hao F and Jiao X: Epigallocatechin gallate (EGCG) suppresses epithelial-Mesenchymal transition (EMT) and invasion in anaplastic thyroid carcinoma cells through blocking of TGF-β1/Smad signaling pathways. Bioengineered 10: 282-291, 2019.
31. Werner TA, Forster CM, Dizdar L, Verde PE, Raba K, Schott M, Knoefel WT and Krieg A: CXCR4/CXCR7/CXCL12 axis promotes an invasive phenotype in medullary thyroid carcinoma. Br J Cancer 117: 1837-1845, 2017.
32. Yang Z, Yu W, Huang R, Ye M and Min Z: SIRT6/HIF-1α axis promotes papillary thyroid cancer progression by inducing epithelial-mesenchymal transition. Cancer Cell Int 19: 17, 2019.